Paper 150

AN EFFECTIVE TOOL FOR THE AUTOMATED GENERATION OF AEROFOIL CHARACTERISTICS TABLES FOR ROTORCRAFT ANALYSIS AND DESIGN

Ngoc Anh Vu*, Jae-Woo Lee*, Sangho Kim*
* Department of Aerospace Information Engineering, Konkuk University
1 Hwayang-dong, Gwangjin-gu, Seoul 143-701, Korea
Corresponding author's email: jwlee@konkuk.ac.kr

Abstract

Rotor performance analysis and design are complex due to the wide variation in flow characteristics. Design tools that can rapidly and accurately compute aerofoil data are needed for rotorcraft design and analysis purposes. A process that effectively automates the generation of two-dimensional (2D) aerofoil characteristics tables has been developed. The process associates a number of commercial software packages and in-house codes that employ diverse methodologies including the Navier–Stokes equation-solving method, the high-order panel method and Euler equations solved with the fully coupled viscous–inviscid interaction (VII) method. This paper describes the development of a general automated generation method that extends from aerofoil shape generation to aerofoil characteristic analysis. The generated data are stored in C81 aerofoil characteristics tables for use in comprehensive rotorcraft analysis codes and rotor blade design. In addition, the methodology could be easily applied for fixed-wing analysis and design, especially for transonic aircraft. The method is demonstrated to achieve aerofoil characteristics quickly and accurately. Calculations for the SC1095 aerofoil section are presented and compared with existing experimental C81 data and previous studies. Guidelines for the use of the process in diverse analyses and designs are also discussed.
Keywords: Automation; Aerofoil characteristics; Rotorcraft Design; Rotor blades Design

Nomenclature

M	Mach number
Re	Reynolds number
α	angle of attack
C_l, C_d, C_m	lift, drag, moment coefficients

Subscripts

α	derivative with respect to angle of attack
∞	freestream quantities
0	zero-lift quantities

Abbreviations

SA	Spalart–Allmaras turbulence model
AoA	angle of attack
CFD	computational fluid dynamics
2D	two-dimensional
RANS	Reynolds Averaged Navier–Stokes
VII	vicous/inviscid interaction

1. INTRODUCTION

The aerodynamics of helicopter rotor blades is a complex discipline. Diverse regimes of flow occur on blades such as reverse flow, subsonic flow, transonic flow, and even supersonic flow. In forward flight, a component of the free stream adds to or subtracts from the rotational velocity at each part of the blade. The blade pitch angle and blade flapping as well as the distribution of induced inflow through the rotor will all affect the blade section angle of attack (AoA) [1]. The non-uniformity of AoA over the rotor disk in conjunction with the inconstant distribution of velocity along the helicopter rotor blade makes aerodynamic analysis difficult.

Comprehensive rotorcraft analysis requires computing the performance, loads, response, and stability of arbitrary rotorcraft configurations [2]. These comprehensive codes utilize look-up tables to provide 2D aerodynamic characteristics, which are then corrected by a number of theoretical and empirical factors for sweep, unsteady aerodynamics, tip-loss factor, etc. These tables, so-called C81 aerofoil characteristics tables, are a text file that contains the lift, drag, and pitching moment coefficients that account for viscous and compressible effects for an aerofoil over extensive ranges of AoA and M_∞. Typically, AoA from -180 deg to 180 deg and M_∞ from 0.0 to 1.0 are presented.

Reliable determination and assessment of the accuracy of aerodynamic data generated in wind tunnels remains one of the most vexing problems in aeronautics. Aerodynamic results are seldom duplicated in different facilities to the level of accuracy that is required either for risk-free engineering development or for the true verification of theoretical and numerical methods [3]. At high AoA (post-stall angle) and high M_∞ ($1 > M_\infty > 0.55$), the measurements of the lift, drag and moment coefficients still remain especially difficult and expensive. On the other hand, very few aerofoil sections have been tested over the entire 360 AoA and Mach number ranges because of the high cost of wind tunnel tests. Therefore, these C81 tables are usually a combination of wind tunnel data, empirical data and numerical analyses data.

For instance, McCroskey proposed an empirical equation for the lift curve slope multiplied by the Prandtl–Glauert corrections in a limited range for the NACA 0012 [3]:

McCroskey attempted to extract as much useful, quantitative information as possible from critical examination and correlations of existing data obtained from over 40 wind tunnel tests. Therefore, this method is not applicable to a large number of new generations of aerofoil shapes.

Marilyn J. Smith et al. evaluated computational fluid dynamics (CFD) codes such as OVERFLOW, FUN2D, CFL3D, Cobalt LLC, and TURNS [4–8] to determine 2D aerofoil characteristics. These CFD computations are found to be as good as experimental data in predicting many of the aerodynamic performance characteristics [9].

With the advancement of computer technology, E.A. Mayda and C.P. Dam developed a CFD-based methodology that automates the generation of 2D aerofoil performance tables [10]. The method employs ARC2D code, which controls a 2D Reynolds-Averaged Navier–Stokes (RANS) flow solver. The choice of flow condition, Mach number and AoA pairs can have a large effect on the C81 table generation time. The valuable capability of this method is to analyze rotor sections at transonic flow where the aerodynamic characteristics of 2D aerofoils are non-linear. Consequently, the choice of Mach number and AoA pairs should be sufficient to ensure the accuracy of the tables for use in comprehensive rotorcraft analysis codes. Fig. 1 shows the average time required to run a case to completion. The research showed that tables containing roughly 400 cases could be completed in 16 hours if 212 processors or more (32-bit AMD Athlon MP 1900+ processors, 1.6 GHz clock speed) are used.

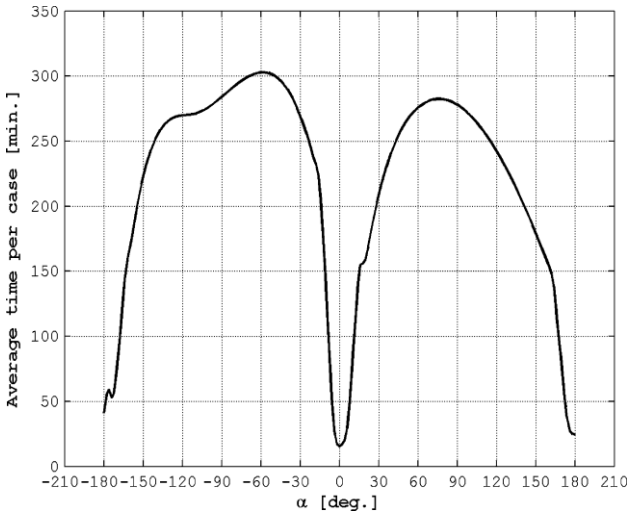

Fig. 1. Smoothed average time required to finish a case as a function of the AoA [10].

The method was shown to perform well for the largely "hands-off" generation of C81 tables, for use mainly in comprehensive rotorcraft analysis codes. Nevertheless, the state of the art of rotorcraft studies is not only for analysis but also for design. The method is a very expensive approach for rotorcraft analysis and design purposes where designers aim to compromise on many factors (design variables) to construct a certain objective. Normally, the optimization process like the one shown in Fig. 2 would perform thousands of iterations to seek the optimum point. The aerofoil shape is governed by several design variables, thus the number of 2D aerofoil analyses could be in the thousands. Therefore, the method proposed by Mayda is not appropriate for design purposes.

The lack of less expensive analysis methods has been blocking multi-variable consideration of rotor blade design optimization. Therefore, rotor blade aerofoil shapes and platforms are usually examined in isolated design optimizations.

Vu et al.'s efforts [11] have performed a rotor blade aerofoil shape and platform in one optimal design problem with the assumption that the helicopter flies at an endurance speed and consequently assuming that the flow field on the blade is subsonic. The study could not examine the optimization design completely. The transonic flow, which is a critical aspect of helicopter aerodynamics, could not be considered appropriately.

An effectively automated approach that is less expensive could contribute greatly to the rapid generation of C81 tables, to provide the ability to consider all aerodynamic aspects in rotor blade design optimization.

This paper describes the development of a methodology that integrates a number of commercial software components and in-house codes that employ diverse methods including the 2D RANS equation-solving method, a high-order panel method, and Euler equations solved with the fully coupled viscous–inviscid interaction method.

The sequent applications of each method are as follows:

- A high-order panel with the fully coupled viscous–inviscid interaction method for
- The Euler equations solved with the fully-coupled viscous–inviscid interaction method for
- The 2D RANS equation-solving method for .

The 2D RANS method is only used for where the two less expensive methods (Euler equations and the high-order Panel solved with the fully coupled viscous–inviscid interaction method) are less suitable.

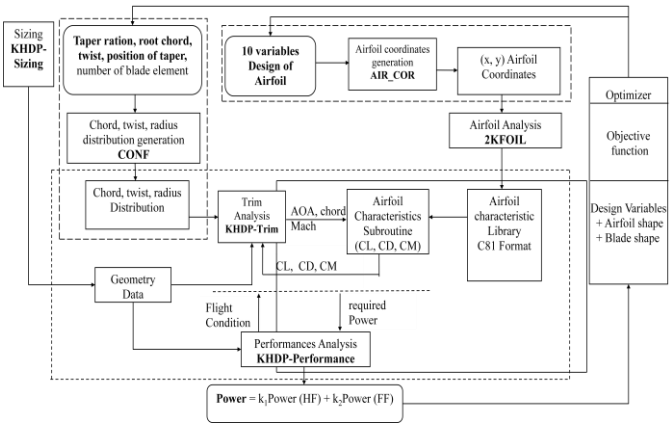

Fig. 2. The design synthesis process [11].

By integrating commercial software and in-house codes, a fully automated process has been developed for generating C81 tables quickly and accurately for arbitrary aerofoil shapes. Moreover, the commercial software including Gridgen V15 and Fluent 6.3.26, used for mesh generation and CFD modeling, are very common in the CFD research community. Therefore, the proposed method could be applicable to any automation process employing Gridgen and Fluent in particular as well as CFD tools in general.

The SC1095 that is used in the UH-60A main rotor was chosen for validation purposes because of the wealth of data available from the UH-60A Airloads flight test programme

[12], as well as the current evaluation of the UH-60A rotor loads by a number of researchers.

2. METHODOLOGY

This section describes the process for automating the generation of aerofoil characteristics, eliminating the need for user inputs and manual operations. Fig. 3 shows the total automated process for aerofoil characteristic estimation.

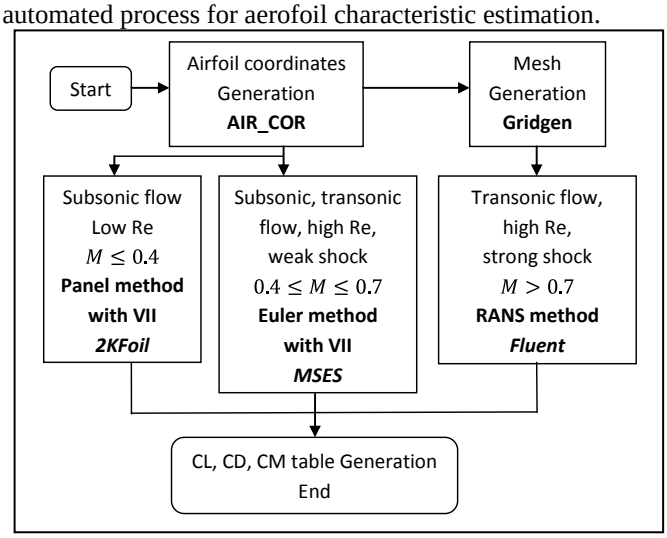

Fig. 3. Automated process of 2D aerofoil characteristics estimation.

2.1 The main steps of the process

a) Aerofoil coordinates generation

An aerofoil coordinates generation code, the so-called AIR_COR, was developed. There are a number of aerofoil representation methods such as Bezier, PARSEC, CST, etc. [13–15]. The AIR_COR code has been implemented for NACA series representations and the recent CST method where the aerofoil shape is governed by a number of parameters. However, it would be straightforward to implement it for other methods. The aerofoil coordinates are stored in text files.

b) Mesh generation

The mesh generations must be automated in order to implement the whole process. Gridgen V15, a software system for the generation of three-dimensional (3D) grids and meshes [16], was employed to generate the 2D aerofoil mesh. The selected software is universally utilized by CFD research and the industrial communities, thereby ensuring that the applications are pertinent and easy for the community.

Gridgen's implementation of Glyph includes the ability to journal the commands executed during an interactive session to provide a starting point for the parametric regeneration of meshes [17]. A pattern of the process of 2D aerofoil mesh generation is journalled by a Tcl-based scripting language (Glyph).

In this study, the aerofoil coordinates stored in a text file is imported by Glyph syntax as:

gg::dbImport "H:/AcademicData/Papers/FGR.DAT" -type SEG

The journal file is then executed by a Batch file having syntax as:

C:\Progra~1\pointw~1\gridge~1\win32\bin\Gridgen.exe -b H:\Academ~1\Papers\2dmesh.glf

In this study, the 2D aerofoil section and surrounding flow domain were discretized using a 405×75 C grid. Fig. 4(a) and Fig. 4(b) show the grid's near-field and trailing-edge regions, respectively. The near-field is densely gridded to capture shocks, shedding vortices, etc. adequately.

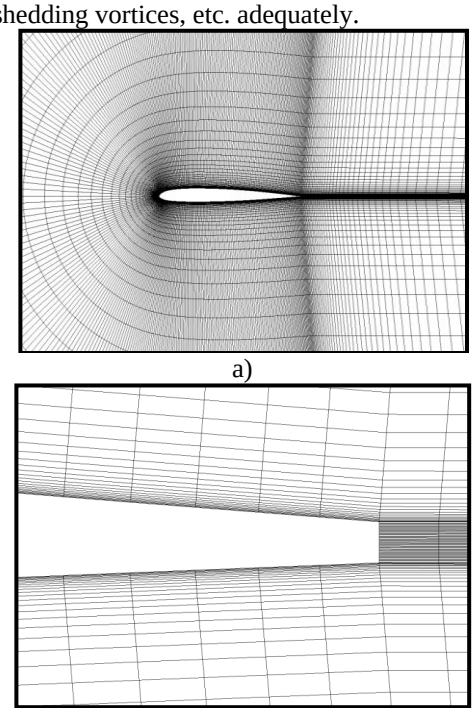

a)

b)

Fig. 4. C-grid for the SC1095 rotor section automatically generated by Gridgen's journal file.

c) Allocation of flow solvers

After obtaining the aerofoil coordinates, the three solvers run, generating the aerofoil characteristics within a user specified range of M_∞ and AoA.

Panel with VII method for : An aerofoil analysis program, 2KFoil, was developed for subsonic isolated aerofoils. The code was adapted from the well known XFOIL code so as to be suitable for the present study. The code employs a simplified envelope version of the e^n method for predicting transition locations. The user-specified parameter "Ncrit" is set to 9.0 (the ambient disturbance level of an average wind tunnel) for all of the predictions [18].

A sequence of AoA from -20 deg to 20 deg is calculated for each M_∞ from 0.05 to 0.4. The starting AoA of each calculation is set to zero deg, and the AOA step is set to 0.5 deg, thereby ensuring that the Newton solution method using the last available solution as a starting guess for a new solution works well [18]. Moreover, an algorithm has been implemented in order to recognize any impossible predictions such as a very high AoA over the stall condition. Detected errors are handled by halting the calculation and proceeding to the next calculation at another M_∞. Therefore, the algorithm ensures good predictions and always completes sequence calculations automatically.

Euler equations with the VII solving method for : MSES, a coupled viscous/inviscid Euler method for a single aerofoil section and multiple sections design and analysis [19] was employed to predict aerofoil characteristics from M_∞ = 0.4 to M_∞ = 0.7.

The in-house code shown in Fig. 5 has been developed to manage the MSES run.

Several solver programs are included in the MSES 3.00 program. This study employs MPOLAR, which is a version of MSES. MPOLAR conveniently sweeps through the range of a specified parameter, thus generating a polar curve [20]. A sequence of AoA from -20 deg to 20 deg is calculated for each M_∞ from 0.4 to 0.7.

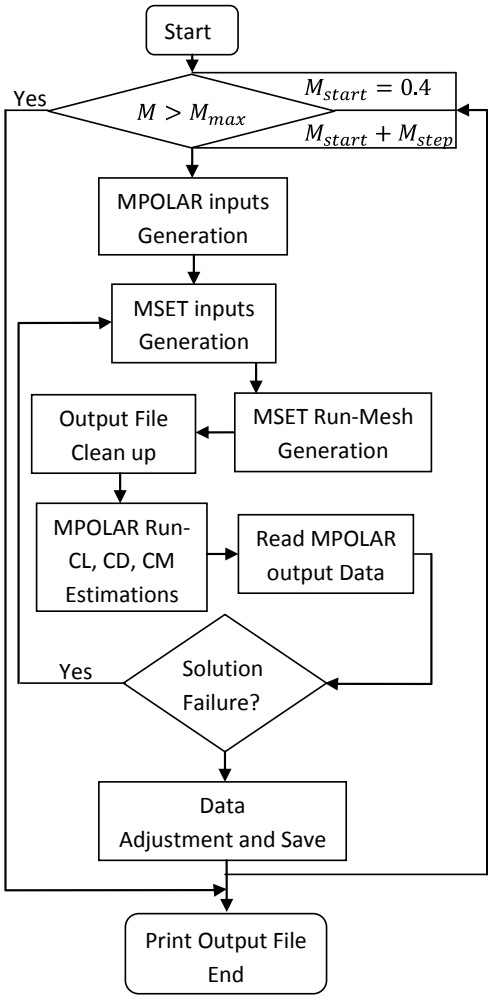

Fig. 5. The automatic process of MSES execution.

Corresponding to each M_∞, an input file for the MPOLAR run is generated. Sequential commands are recorded in a text file and played back when MSET is run in DOS mode. MSET is the program that initializes the grid, the flow field and a variety of other variables [20]. Those variables are utilized to run the MPOLAR solver. An analysis of the output file data is performed in order to check the success of the calculation. If the solution fails, the above process is restarted from the generation of inputs for MSET. Otherwise, the output data are adjusted to comply with the user-defined format and another calculation for the next M_∞ proceeds.

RANS equation solving for : Fluent 6.3.26, comprehensive software for CFD modelling, was employed to analyze 2D aerofoil characteristics in the transonic region. The software is widely utilized by CFD research and industries, thereby ensuring that the development is applicable to the community. Moreover, it would be straightforward to support for other solvers.

An in-house code shown in Fig. 6 has been developed to manage the Fluent run. A library of journal files that are utilized for the run of the case setting AoA = 0 deg is created. For instance, the journal files are created for the following M_∞ and AoA pairs: M_∞ = 0.75, AoA = 0 deg; M_∞ = 0.80, AoA = 0 deg; M_∞ = 0.85, AoA = 0 deg; etc. A journal file contains a sequence of Fluent commands, arranged as they would be typed interactively into the program or entered through a GUI. The GUI commands are recorded as scheme code lines in journal files [21].

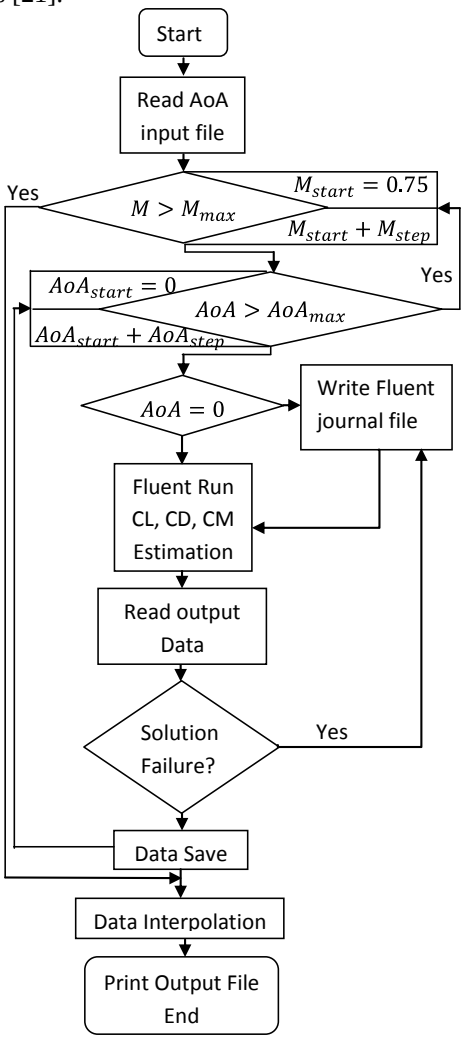

Fig. 6. Automatic process of Fluent execution.

The AoA are defined in an input file. Corresponding to each M_∞, a sequence of AoA is calculated. The initiation of each calculation uses the last available solution so that the convergence of the current solution can be much faster. The library journal file is utilized to run the Fluent solver if AoA = 0 deg. Otherwise, a new journal file is generated and the Fluent solver is performed. The calculation for each M_∞ is started when the preceding M_∞ has completed the calculation for AoA = 0 deg, as shown in Fig. 7. An analysis of the output file data is performed in order to check the success of the calculation. If the solution fails, the Fluent solver is restarted by changing the solver inputs via the journal file. Otherwise, the data are saved and another calculation for the next AoA is commenced. The data are interpolated for uncalculated regions before generating the output file.

The jounal files are executed by Batch files having syntax as: *C:\Fluent.Inc\ntbin\ntx86\Anh\jour_lib\fluent 2d -g -wait -i C:\Fluent.Inc\ntbin\ntx86\Anh\jour_lib\M75AP000*

As shown in the syntax, the process waits for the completion of Fluent execution. The Fluent GUI is closed upon completion by adding the command "exit yes" to the end of each journal file.

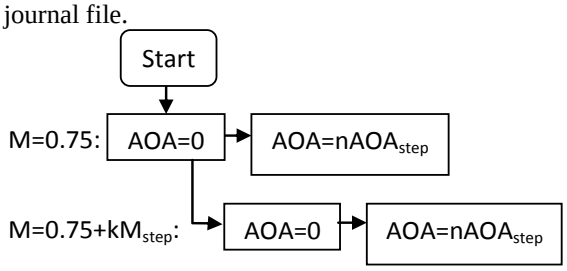

Fig. 7. Sequence runs of the Fluent solver.

2.2 Flow solver

The three flow solvers chosen for the development of the automated process are 2KFoil, MSES and Fluent. A sequence of the most expensive to the least expensive solvers is RANS, Euler and Panel. It is desirable to use the least expensive solver as much as possible.

a) 2KFoil

The 2KFOIL is an aerofoil analysis program for subsonic isolated aerofoils adapted from the XFOIL code. The main algorithm of this code is a combination of high-order panel methods with a fully coupled viscous/inviscid interaction method. The inviscid formulation of XFoil is a linear vorticity stream function panel method. A Karman–Tsien compressibility correction is incorporated, allowing good compressible predictions. The viscous formulations come from the boundary layers and wake, which are described with a two-equation lagged dissipation integral boundary layer and an envelope e^n transition criterion. Transition in an XFOIL solution is triggered by one of two ways: free transition or forced transition. The user-specified parameter "Ncrit" is set to 9.0 (the ambient disturbance level of an average wind tunnel) for all of the predictions [18].

The ASEQ command in OPER is applied to increase the AoA gradually; the AoA step size is set to 0.5. When performing viscous analysis calculations, it is always a good idea to sequence the runs so that the alpha does not change too drastically from one case to another. The Newton solution method always uses the last available solution as a starting guess for a new solution, and works best if the change from the old to the new solution is reasonably small [18].

The methodology is able to perform analysis for diverse aerofoil shapes. Thus all solvers must be robust to predict aerofoil characteristics. For a typical helicopter, on the advancing blade at a point where the M_∞ is 0.4 the Re will be as high as . When M_∞ is greater than 0.4, the compressibility becomes significant, and the Re becomes a very high number where the accuracy of the method depreciates. Therefore, the use of 2KFoil is up to $M_\infty = 0.4$.

b) MSES

A method for accurately calculating transonic aerofoil flow is implemented in the viscous/inviscid design analysis code MSES. The Euler equations are discretized on a conservative streamline grid and are strongly coupled to a two-equation integral boundary-layer formulation using the displacement thickness concept. A transition prediction formulation of the e^9 type is derived and incorporated into the viscous formulation. The entire discrete equation set, including the viscous and transition formulations, is solved as a fully coupled non-linear system by a global Newton method [22].

Drela evaluated the method for an RAE 2822 aerofoil at deg. Good greement with experimental results was obtained [22]. However, it was subsequently found that the method is not robust when the shock occurring on the aerofoil becomes strong. When the AoA increases, the boundary layer might be separated and the solution might not converge. To ensure the robustness of the method for all cases of aerofoil shape, the method is utilized to predict for M_∞ from 0.4 to 0.7.

c) Fluent

Fluent 6.3.26 is comprehensive software for CFD modelling. The current study utilized the 2D mode in order to predict 2D aerofoil characteristics.

In this study, the Spalart–Allmaras turbulence model is chosen for the viscous model, the Suntherland Law is chosen for material viscosity and the turbulent viscosity ratio is chosen for the turbulence specification method of pressure far-field.

The method is applied for . The initial calculation typically takes about 300–500 iterations to obtain convergence solutions, and the proceeding calculations typically takes about 100–200 iterations in case the step size for M_∞ is 0.05, and AoA is 0.5 deg.

2.3 Programming languages

The Fortran 77 programming languages were chosen for the development of the automation process. Flow solvers in the CFD field are usually developed in Fortran 77. Most engineers and researchers in the area of aeronautics understand the language. Therefore, the use is convenient and it is easy to develop the integration of a number of solvers. A number of batch jobs are set up so they can be run to completion without manual intervention.

3. RESULTS

The aerodynamic characteristics of the SC1095 aerofoil are presented with reference to the experimental results tabulated by Bousman [24] and the ARC2D results presented by Mayda [10].

3.1 Lift curve slope

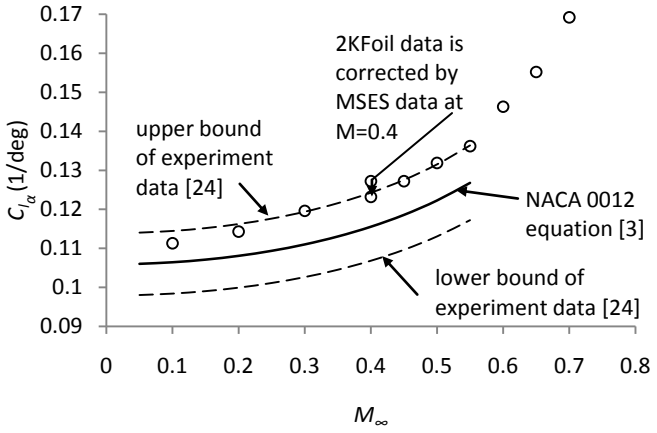

a)

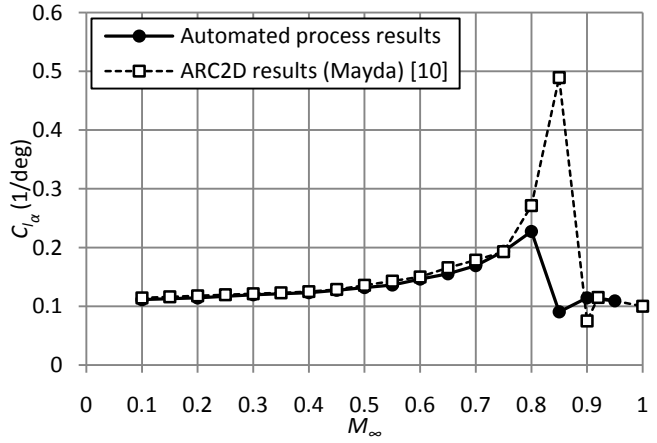

b)

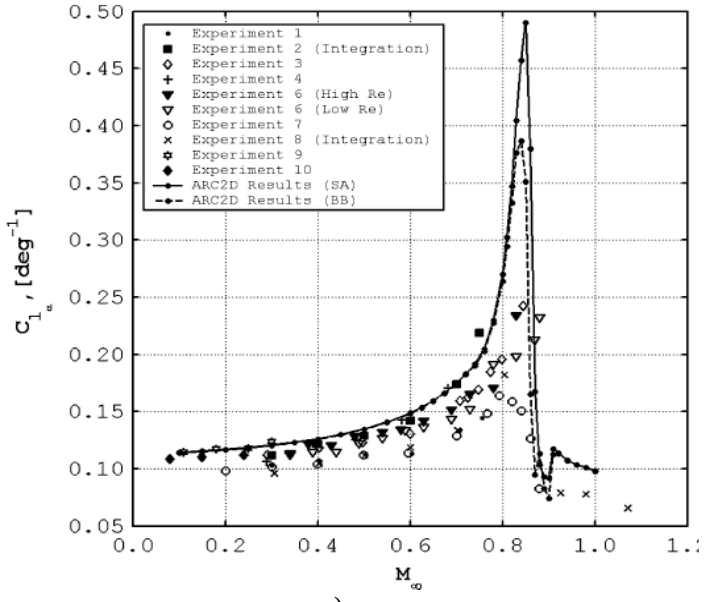

c)

Fig. 8. Lift curve slope at zero lift as a function of M_∞ for the SC1095 aerofoil. a) In comparison with the experimental data obtained by Bousman [24]; b) in comparison with the ARC2D results obtained by Mayda [10]; c) comparison of Mayda

The lift curve slope data at zero-lift conditions of the experiment and the automated process are shown as a function of freestream M_∞ in Fig. 8. It is seen that the automated process generated the data near the upper boundary of the experimental data. The data generated by 2KFoil tends to increase when M_∞ increases. At M_∞ = 0.4, the data are out of the experimental data bound. The Re at this condition is quite high, and consequently the application of the panel method is not appropriate. Therefore, the lift curve slope is calculated by 2KFoil up to M_∞ = 0.4, then corrected by the lift curve slope calculated by MSES at M_∞ = 0.4.

When the SA turbulence model is used, Fluent provides data with lower values than ARC2D. The Fluent data are very close to experiments 3, 6 and 7 in Ref. 24.

3.2 Zero-lift angle of attack

The AoA corresponding to the zero-lift condition for the experiments and the automated process are plotted versus M_∞ in Fig. 9. For , α_0 is nearly constant at -0.75 deg while the experimental data range from -0.1 to -1.0 deg. The deviations in this measurement are evidence of bias errors in measuring the AoA or rigging errors.

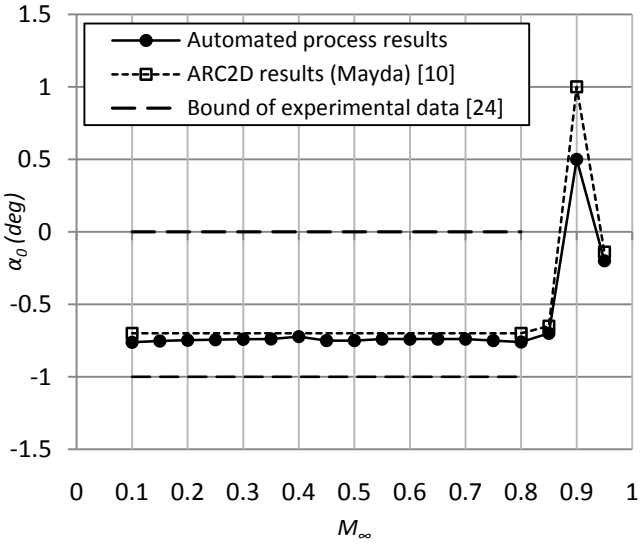

Fig. 9. AoA at zero lift as a function of M_∞ for the SC1095 aerofoil.

3.3 Zero-lift drag coefficient

The zero-lift drag coefficient data of the experiment and automated process are shown in Fig. 10. There is fairly good agreement between the experimental data and the calculated data. Different Re and boundary layer transition locations are likely causes of scatter in the experimental data. The automated process results show good agreement with the experiment in the drag-divergence zone where the drag coefficient sharply increases.

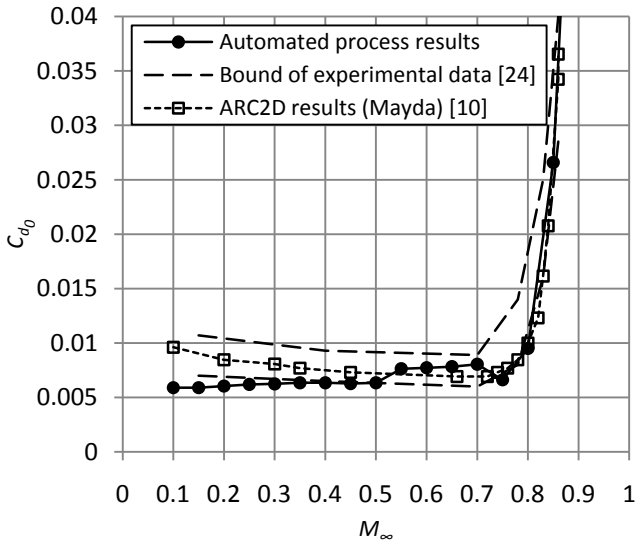

Fig. 10. Drag coefficient at zero lift as a function of M_∞ for the SC1095 aerofoil.

3.4 Zero-lift pitching moment coefficient

The zero-lift pitching moment coefficient versus M_∞ of the experimental data and the automated process results are shown in Fig. 11. The pitching moment coefficient is a difficult quantity to evaluate experimentally as evidenced by the scatter in the plot in Ref. 24.

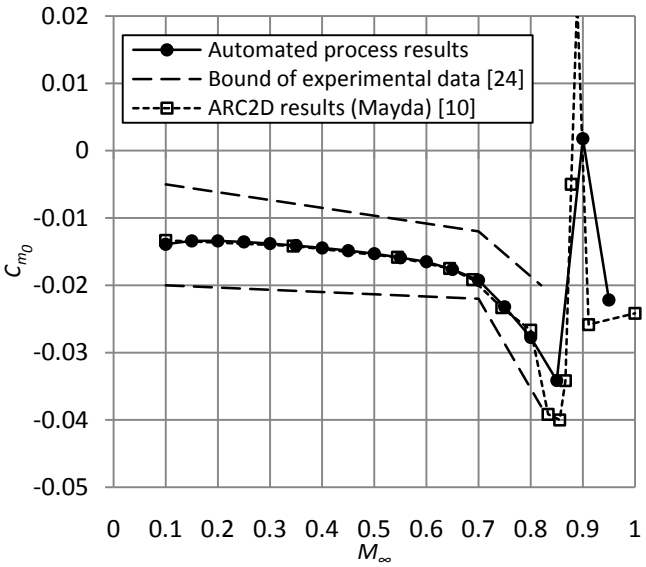

Fig. 11. Zero-lift pitching moment coefficient as a function of M_∞ for the SC1095 aerofoil.

3.5 Pitching moment curve slope

The pitching moment curve slope versus M_∞ of the experimental data and the automated process results are shown in Fig. 12. For , the pitching moment curve slope is nearly constant at 0 deg^{-1} and all the data are in good agreement.

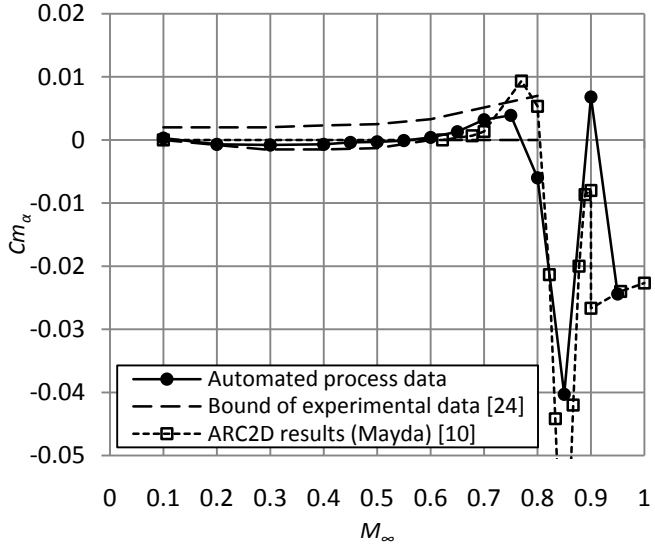

Fig. 12. Pitching moment curve slope at zero lift as a function of M_∞ for the SC1095 aerofoil.

3.6 Maximum lift coefficient and the AoA at the maximum lift coefficient

The maximum lift coefficient versus M_∞ of the experimental data and the automated process results is shown in Fig. 13. Prediction of the maximum lift coefficient for a 2D aerofoil by CFD is a challenging task. It is difficult to model several phenomena installed in a region such as the placement of the laminar-turbulent transition locations and the resolution of laminar separation bubbles very near the leading edge.

The ARC2D results fall within the bounds of the experiment for while the automated process results fall within the bounds for M_∞ up to 0.75.

The AoA at the maximum lift coefficient is an important indicator of stall characteristic predictions. Fig. 14 shows the AoA at the maximum lift coefficient versus M_∞. The data appear near the lower boundary of the experimental data where experiments 6 and 7 in Ref. 24 are obtained. It is a difficult quantity to evaluate, especially in the transonic region. As M_∞ increases the AoA at the maximum lift coefficient decreases.

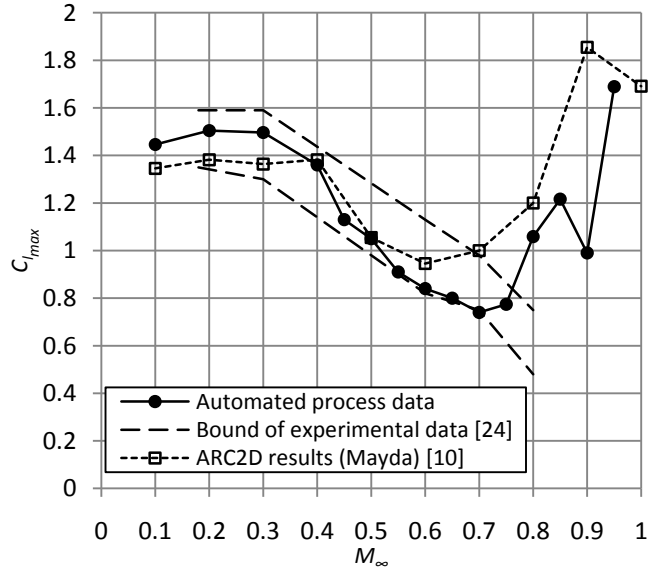

Fig. 13. Maximum lift coefficient as a function of M_∞ for the SC1095 aerofoil.

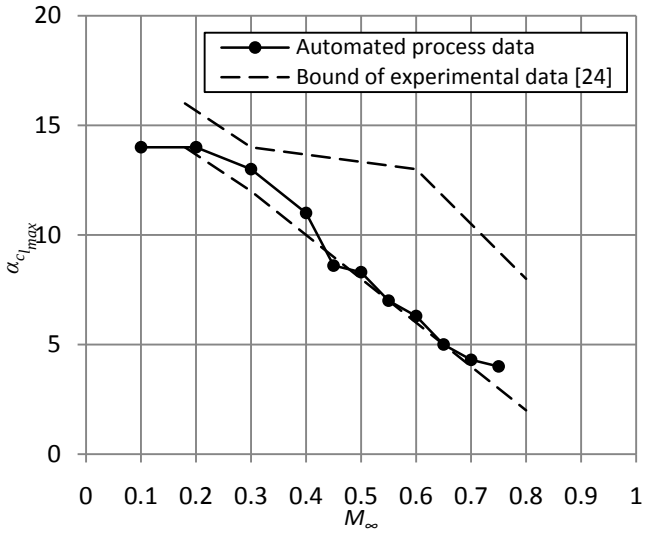

Fig. 14. AoA at the maximum lift coefficient as a function of M_∞ for the SC1095 aerofoil.

3.8 Comparison of computational and existing C81 data

The lift, drag and pitching moment coefficients of the automated process calculation at M_∞ = 0.4 for AoA from -20 deg to 20 deg are shown in Fig. 15.

The automated process results are very close to the ARC2D results. However, the maximum lift coefficient and the AoA at the maximum lift coefficient are important values in helicopter rotor aerofoil design. Therefore, the accuracy of these values has a very important role.

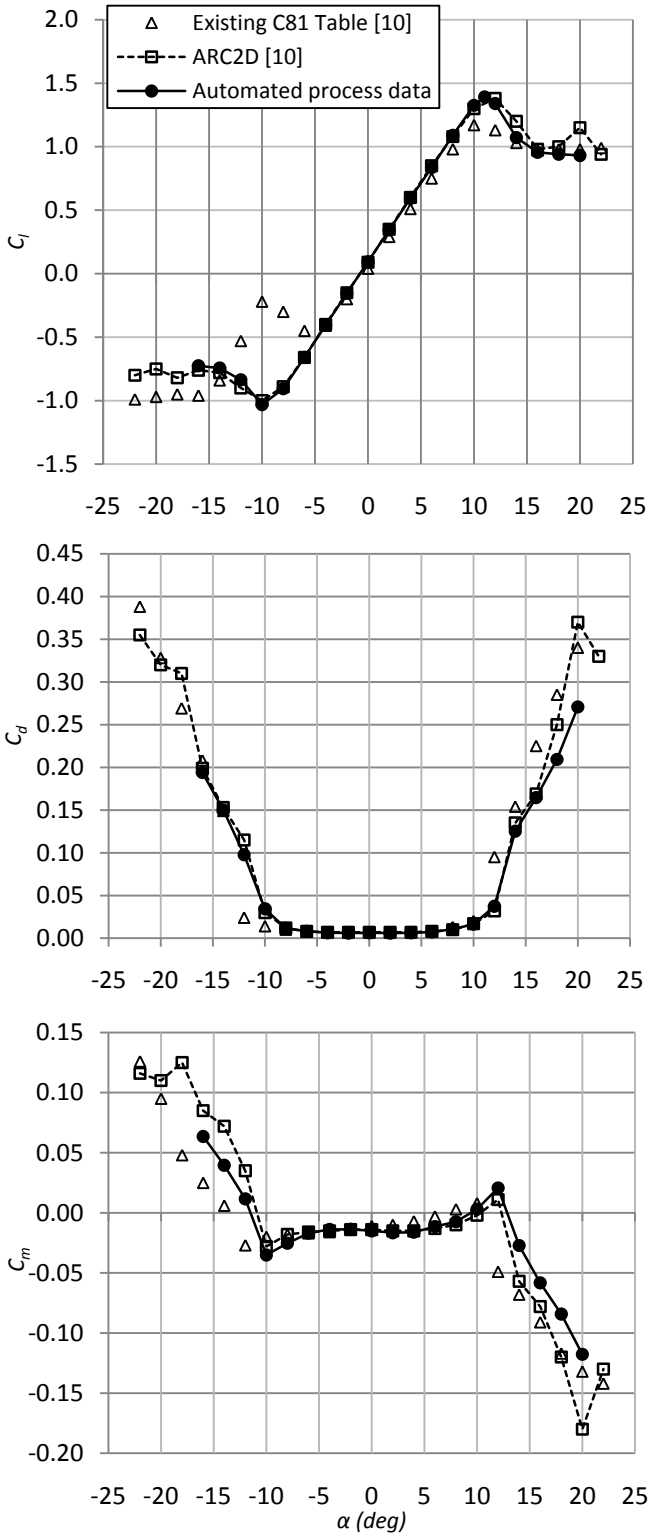

Fig. 15. Lift, drag and moment coefficients at M_∞ = 0.4 for the SC1095 aerofoil.

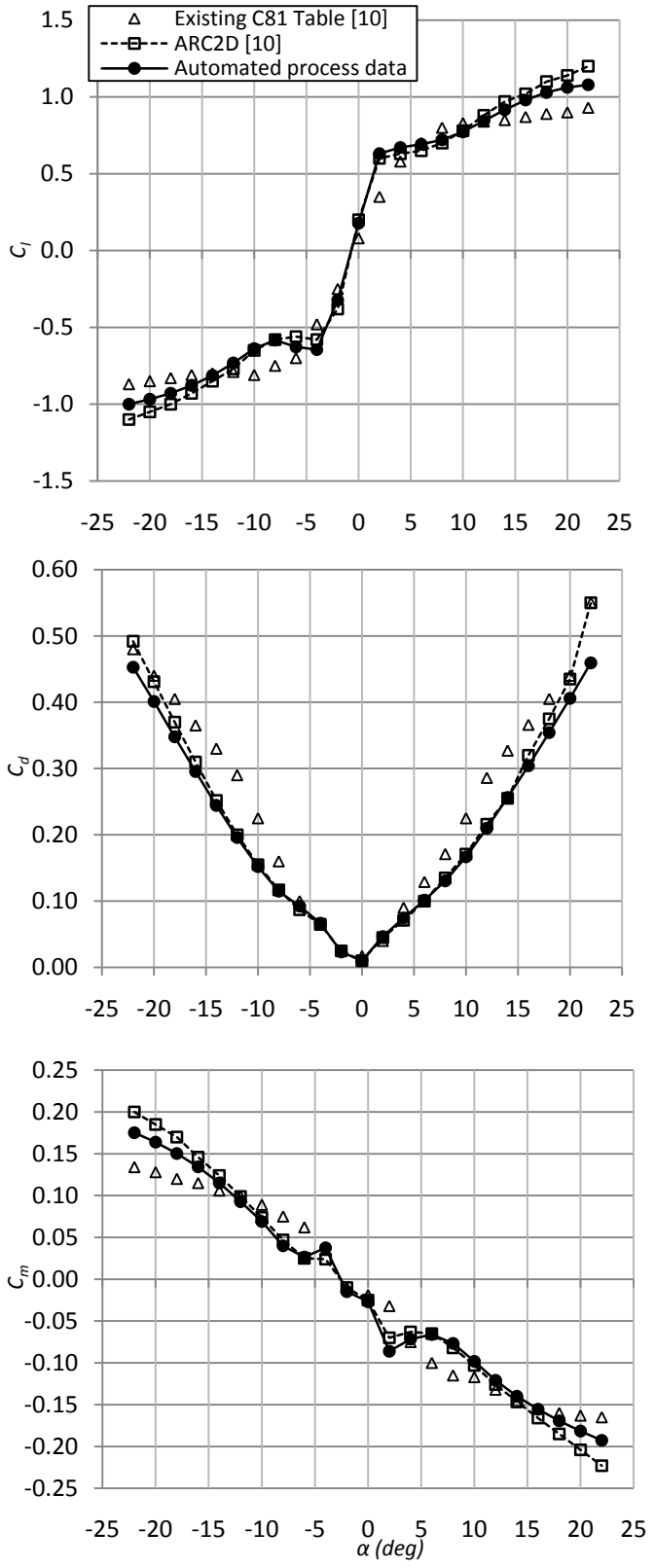

Fig. 16. Lift, drag and moment coefficients at M_∞ = 0.8 for the SC1095 aerofoil.

As shown in Fig. 8, the lift curve slope result at M_∞ = 0.4 of 2KFoil is out of the bounds of the experimental data, thus the results were corrected to be in the bounds by using the MSES curve slope results.

Stall behaviour still remains difficult for CFD researchers. The current study and Mayda's study have the same problem for this region. For other regions, the automated process results and existing C81 table data are in good agreement.

The drag coefficient calculated by the automated process agrees very well with the C81 data as ARC2D.

The existing C81 data and the moment coefficient calculated by the automated process are also in a good agreement.

The lift, drag and pitching moment coefficients of the automated process calculation at M_∞ = 0.8 for AoA from -20 deg to 20 deg are shown in Fig. 16. At this M_∞, Fluent is employed to calculate the 2D aerofoil characteristics.

Both the ARC2D results and the automated process results for the lift curve slope are overpredicted at M_∞ = 0.8. The calculated drag coefficients near AoA = 0 deg are in good agreement. The pitching moment varies non-linearly near AoA = 0 deg because of the shock commencing on the aerofoil.

In general, the ARC2D and automated process results have the same data trend due to using the same SA turbulence model.

4. C81 TABLE GENERATION AND APPLICATION FOR DIVERSE DESIGN AND ANALYSIS

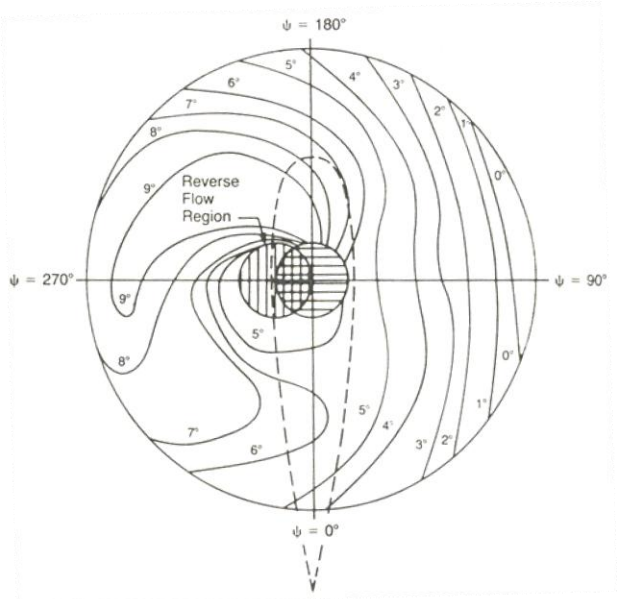

Fig. 17. Angle of Attack Distribution for Example Helicopter at 115knots [25].

Fig. 17 shows AoA distribution of example helicopter at 115knots. In hover and forward flight, the AoA distribution range is between -20 deg and 20 deg and the M_∞ distribution range is from 0 to 1. This covers the majority of helicopter flight conditions. Therefore, the data within those ranges are required to be highly accurate. In this study, the 2D aerofoil characteristics for AoA from -20 deg to 20 deg and M_∞ from 0 to 1 are calculated by diverse codes and software with a high level of accuracy. Outside this AoA range, the flow is often characterized by stalled conditions. None of the theories and computational methodologies can estimate the aerodynamic characteristics accurately. The aerofoil shape has a minor effect on aerofoil aerodynamics, so that the data in the flow

regimes not covered by the solution process are taken from NACA 0012 wind tunnel experiments. Thereafter, the data are combined and written into a text file called C81 tables. The step size of M_∞ is 0.05 and that of AoA is 0.5 deg. The technique not only enhances the convergence of the automated process but also provides more accurate data for the C81 table.

There are many factors affecting the total time to generate the C81 table. These factors include the number of cases (M_∞, AoA pairs), the speed of the processors, grid systems, flow solver models, and the duration of the longest case. These are discussed in Ref. 10. The longest amount of time is required by the RANS method. Thus the treatment of the conditions where the RANS method is applied has a very important role in reducing the total amount of time. The initial calculation using Fluent software required 300–500 iterations while the proceeding calculations required 100–200 iterations to converge. Each iteration requires about 0.4 seconds on a computer having a dual-core, 2.5GHz CPU with 3.00GB of RAM. Solving Panel and Euler equations with VII method require a little time less than 5 seconds for a pair of AoA and M_∞. Because the computationally expensive RANS method is only applied for , the proposed process reduces computational time by 70% when compared to Mayda's process while retaining the same level of accuracy. This advance makes the process applicable for design purposes, where the designers seek to update their aerofoil tables frequently for new designs. Therefore, the use of the process shown in Fig. 7 is particularly suitable for these kinds of analysis.

In this section, the techniques to choose a number of flow conditions in order to reduce the required time for the completion of C81 table generation are discussed. According to each design or analysis of specific rotorcraft, researchers should choose adequate M_∞, AoA pairs to cover the whole flight conditions. Simultaniously, the choices should cover too large a range to avoid causing an expensive time requirement for completion. Consider a helicopter that has a rotor tip speed of 700 ft/s and a maximum forward speed of 150 knots, yielding a maximum M_∞ at the tip of the rotor blade is 0.847. In this case, the M_∞ range should not exceed 0.85.

On the advancing side, the AoA at the tip of the rotor blade is nearly zero deg in a trimmed flight condition so it is not necessary to sweep the AoA in high M_∞ from -20 deg to 20 deg. According to each rotorcraft, the author recommends that the AoA sweeps from -5 deg to 5 deg for high M_∞ at the tip of the rotor blade in general. Therefore, the time required for completion would be significantly reduced. Understanding the design and analysis problem is always the best way to use the automated process effectively.

This process enhances aerofoil shape study and design where the designers desire to quickly manipulate a number of aerofoil shapes applicable for diverse flow (subsonic, transonic, supersonic) on rotor blades, wing, propeller, wind turbines. The process is also applicable to piston and turboprop aircraft propeller design by enabling the rapid analysis of propeller aerofoils.

5. CONCLUSION

This paper describes an effective automated process for generating 2D aerofoil characteristics tables. The process utilizes a number of commercial software packages and in-house codes that employ diverse methods including the Panel, Euler and RANS methods. The pertinence of each method to each flow condition was discussed. The use of each method in an effective manner was also described and remarked upon. A managing in-house code has been developed that allocates the tasks for each solver code and software package, and combines the data into C81 aerofoil characteristics tables.

The application of the automated process was demonstrated and validated for the aerofoil SC1095. The data were compared with the experimental data summarized in Bousman's paper [24], and the data of ARC2D obtained by Mayda [10]. Good agreements with the experimental data were obtained in general.

The method has yielded a computationally inexpensive tool for generating C81 tables for use in comprehensive rotorcraft analysis codes. It is also convenient for researchers because it reduces computational time significantly, yielding short analysis times on personal computers. The longest solution time is from the RANS method. By reducing the number of required RANS evaluations, a 70 percent reduction in computational time was achieved without reducing accuracy. This advance makes the process applicable for rotor blade design where frequent changes to the aerofoil shape may occur.

In general, the automated process that extends from aerofoil shape generation to aerofoil characteristics analysis is a valuable tool for supporting comprehensive rotorcraft analysis codes and rotor blade design in an effective and inexpensive manner. Designers can perform tradeoff studies of aerofoil shapes applied to rotor blades, wings, wind turbines, and propeller quickly.

The use of Gridgen, Fluent commercial software in an automated modelling process could be widely applicable for any other design problems or simulations where the automation is necessary.

ACKNOWLEDGEMENT

This work was supported by the Defense Acquisition Program Administration and the Agency for Defense Development in the Republic of Korea under the contract UD070041AD, and in the project KARI-University Partnership Program 2009-09-2.

REFERENCES

[1] J.G. Leishman, Principles of Helicopter Aerodynamics, second ed., Cambridge Aerospace Series, Cambridge University Press, USA, 2006.

[2] W. Johnson, Rotorcraft Aerodynamics Models for a Comprehensive Analysis, American Helicopter Society 54th Annual Forum, Washington, D.C., May 1998.

[3] W.J. McCroskey, A Critical Assessment of Wind Tunnel Results for the NACA 0012 Airfoil, NASA Technical Memorandum 100019, USAAVSOM Technical Report 87-A-5, October 1987.

[4] P.G. Buning, D.C. Jespersen, T.H. Pulliam, W.M. Chan, J.P. Slotnick, S.E. Krist, K.J. Renze, OVERFLOW User's Manual, Version 1.8s, NASA Langley Research Center, 1998.

[5] W.K. Anderson, D.L. Bonhaus, An implicit upwind algorithm for computing turbulent flows on unstructured grids, Comput. and Fluid, 23 (1) (1994) 1–21.

[6] C. Rumsey, R. Biedron, J. Thomas, CFL3D: Its History and Some Recent Application, NASA TM-112861, May 1997.
[7] W.Z. Strang, R.F. Tomaro, M.J. Grismer, The Defining Methods of Cobalt60: A Parallel, Implicit, Unstructured Euler/Navier-Stokes Flow Solver, AIAA 99-0786, 1999.
[8] G.R. Srinivasan, J.D. Baeder, TURNS: A free wake Euler/Navier-Stokes numerical method for helicopter rotors, AIAA J., 31 (5) (May 1993).
[9] M.J. Smith, T.C. Wong, M.A. Potsdam, J. Baeder, S. Phanse, Evaluation of computational fluid dynamics to determine two-dimensional airfoil characteristics for rotorcraft applications, J. Am. Helicopter Soc., 51 (1) (2006) 70–79.
[10] E.A. Mayda, C.P. van Dam, Automated generation of airfoil performance tables using a two-dimensional Navier-Stokes solver, J. Am. Helicopter Soc., 50 (4) (Oct. 2005) 338–348.
[11] N.A. Vu, J.W. Lee, Y.H. Byun, S.H. Kim, Aerodynamic Design Optimization of Helicopter Rotor Blades Including Airfoil Shape, 66th Annual Forum of the American Helicopter Society, Pheonix, AZ, May 2010.
[12] W.G. Bousman, R.M. Kufeld, D. Balough, J.L. Cross, K.F. Studebaker, C.D. Jennison, Flight Testing the UH-60A Airloads Aircraft, 50th Annual Forum of the American Helicopter Society, Washington, D.C., May 1994.
[13] K.W. Anderson, D.L. Bonhaus, Airfoil design on unstructured grids for turbulent flows, AIAA J., 37 (2) (February 1999) 185–191.
[14] H. Sobieczky, Parametric airfoil and wings, notes on numerical fluid mechanics, Vieweg (1997) 71–88.
[15] B.M. Kulfan, A Universal Parametric Geometry Representation Method – "CST", AIAA-2007-62, 45th AIAA Aerospace Sciences Meeting and Exhibition, Reno, Nevada, USA, 8–11 January 2007.
[16] Gridgen, User Manual, Version 15, Pointwise, Get the Point, 2003.
[17] http://www.pointwise.com/archive/rn14-01-R1.shtml.
[18] M. Drela, H. Youngren, XFOIL 6.94 User Guide, MIT Aero & Astro, 10 December 2001.
[19] http://www.am-inc.com/PDF/MSES.pdf.
[20] M. Drela, A User's Guide to MSES 3.00, MIT Department of Aeronautics and Astronautics, March 2004.
[21] Fluent Inc., FLUENT 6.3 User's Guide, Centerra Resource Park, 10 Cavendish Court, Lebanon, NH 03766, September 2006.
[22] M. Drela, M.B. Giles, Viscous-inviscid analysis of transonic and low Reynolds number airfoils, AIAA J., 25 (10) (Oct. 1987) 1347–1355.
[23] http://en.wikipedia.org/wiki/Batch_processing.
[24] W.G. Bousman, Aerodynamic Characteristics of SC1095 and SC1094 R8 Airfoil, NASA/TP-2003-212265, AFDD/TR-04-003, Ames Research Center, Moffett Field, California 94035-1000, December 2003.
[25] R. W. Prouty, Helicopter Performance, Stability, and Control, PWS Engineering Boston, USA, 1986